Nonadditivity in the effective interactions of binary charged colloidal suspensions

E Allahyarov[1,2], H Löwen[1]

[1] Institut für Theoretische Physik II: Weiche Materie, Heinrich-Heine-Universität Düsseldorf, Universitätsstraße 1, D-40225 Düsseldorf, Germany

[2] Department of Physics, Case Western Reserve University, Cleveland, Ohio 44106, USA, and Joint Institute for High Temperatures, Russian Academy of Sciences, Moscow, Russia

E-mail: elshad.allakhyarov@case.edu

Abstract. Based on primitive model computer simulations with explicit microions, we calculate the effective interactions in a binary mixture of charged colloids with species A and B for different size and charge ratios. An optimal pairwise interaction is obtained by fitting the many-body effective forces. This interaction is close to a Yukawa (or Derjaguin-Landau-Verwey-Overbeek(DLVO)) pair potential but the AB cross-interaction is different from the geometric mean of the two direct AA and BB interactions. As a function of charge asymmetry, the corresponding nonadditivity parameter is first positive, then getting significantly negative and is getting then positive again. We finally show that an inclusion of nonadditivity within an optimal effective Yukawa model gives better predictions for the fluid pair structure than DLVO-theory.

PACS numbers: 82.70.Dd, 61.20.Ja

Submitted to: *J. Phys.: Condens. Matter , special issue*

1. Introduction

Phase diagrams and structural correlations in binary mixtures are much richer than those of their one-component counterparts [1] since there are additional thermodynamic degrees of freedom. Understanding the phase behaviour from first principles [2, 3] requires the knowledge of the effective interaction forces between the different species which is - in general - a many-body force. Even if this interaction is pairwise additive, the full calculation of structure and phase behaviour has only been done for selected cases. Among those are hard spheres [4, 5, 6, 7], oppositely charged colloids [8, 9], two-dimensional dipolar mixtures [10, 11] and two-dimensional Yukawa mixtures [12].

In this paper we consider a three-dimensional binary colloidal suspension of two species A and B of charged spheres ("macroions") with different charges (Z_Ae and Z_Be, e denoting the electron charge) and diameters (σ_A and σ_B) [13, 14, 15]. The traditional Derjaguin-Landau-Verwey-Overbeek (DLVO) theory describes the interaction between the two species as an effective pairwise Yukawa potential [16, 17]

$$V(r) = \frac{Z_i e}{1+\sigma_i\kappa_D/2}\frac{Z_j e}{1+\sigma_j\kappa_D/2}\frac{\exp(-\kappa_D(r-(\sigma_i+\sigma_j)/2))}{\epsilon r} \tag{1}$$

where $(ij) = (AA), (AB), (BB)$, ϵ denotes the dielectric constant of the solvent and κ_D is the Debye-Hückel screening parameter. The latter is given as

$${\kappa_D}^2 = 4\pi(\sum_j z_j^2\rho_j)/\epsilon k_B T \tag{2}$$

where the sum runs over all microions with their charges z_j and partial number densities ρ_j. The DLVO theory is a linearized theory and therefore neglects nonlinear screening effects [19, 18] which give rise to effective many-body forces [20, 21, 22, 23, 24]. Nonlinear effects can at least partially be accounted for by charge renormalization which is conveniently calculated in a spherical Poisson-Boltzmann cell model [25]. The cell approach was recently generalized towards binary mixtures by Torres, Téllez and van Roij [26]. In the latter approach, it was shown that charge renormalization is different for the different species such that the ratio of effective charges is different from that of the bare charge. However, the cross-interaction was not addressed in this study.

The importance of the cross-interaction between A and B relative to the direct part AA and BB determines the so-called non-additivity parameter Δ of the mixture which is crucial for the topology of phase diagrams. Binary hard sphere systems have been studied as a prototype for any non-additive mixtures [27, 28, 29]. In general, a positive non-additivity is realized if the cross-interaction is more repulsive than the mean of the two direct interactions. For high positive non-additivity ($\Delta > 0$), macrophase separation into an A-rich and B-rich phase is observed, i.e. the system minimizes the interface where the AB cross-interactions plays a dominant role. The other case of negative nonadditivity ($\Delta < 0$) implies a weaker cross-interaction in terms of the bare ones such that the system tends to mix and to exhibit micro-phase-separation [30].

For pairwise Yukawa interactions $V_{ij}(r) = {Z_{ij}^*}^2\exp(-\kappa_D r)/r$ $((i,j) = (AA), (AB), (BB))$, a dimensionless nonadditivity parameter Δ can be quantified by

invoking the deviation of an ideal Berthelot mixing rule [31, 32] via the relation

$$1 + \Delta = {Z_{12}^*}^2 / Z_{11}^* Z_{22}^* \tag{3}$$

For charged suspensions, classical DLVO theory (see eqn. (1)) implies a vanishing Δ since the effective charges are the same in all interactions. There are other realizations of a binary Yukawa system in dusty plasmas [33, 34, 35] and metallic mixtures [36] or amorphous silica [37]. In fact, the binary Yukawa model has been widely used and employed to investigate effective interactions [38], fluid-fluid phase separation [39, 40, 41], vitrification [42, 43, 44, 45, 46] and transport properties [47]. In most of studies of binary Yukawa systems, the non-additivity parameter is set to zero, except for Refs. [31, 32] where the effect of positive nonadditivity Δ on fluid-fluid phase separation is considered. In the context of dusty plasmas, there is another recent study showing that the non-additivity parameter Δ is positive in general [48]. This leads to macrophase separation in binary dusty plasmas, as observed in experiments [35, 48]. The physical origin of the interaction in dusty plasmas, however, is different from that relevant for charged colloidal suspensions. While for the former the ion are described by a Gurevich distribution, a Boltzmann distribution is appropriate for the latter.

In this paper, we focus on the nonadditivity of the cross-interaction for charged colloidal suspensions. Using computer simulations with explicit microions [49, 50, 51, 52], we calculate the effective interactions in a charged binary mixture and find that the sign of the non-additivity depends on the parameters, in particular on the charge asymmetry. The nonadditivity parameter is calculated first by using simulations of three pairs of macroions, namely AA, AB, and BB in a periodically repeated simulation box at fixed screening. We also consider larger systems with 24 macroions at different compositions in order to check the effect on many-body forces on Δ. In the latter case we fit the many-body forces by effective pairwise forces $-dV_{ij}(r)/dr$ and extract Δ from the optimal fit [53]. We confirm that Δ is unchanged. Our main findings are i) that Δ is typically large and cannot be neglected and ii) that the sign of Δ depends on the parameters as e.g. charge asymmetry. If a binary charged colloidal mixture is described by an effective Yukawa model, Δ needs to be incorporated into the description. For instance when compared to DLVO theory a much better description of the fluid pair structure is achieved within an effective Yukawa model and non-vanishing Δ.

The paper is organized as follows: In Sec. II we describe the model and the simulation method and apply it to the case of two macroions. Many-body simulations with 24 macroions are discussed in Sec. III. Then we present data for a large system with effective pairwise Yukawa forces in order to see the effect of non-vanishing nonadditivity in Sec. IV. Finally we conclude in Sec. V.

2. Simulations with two macroions

We model all ions as uniformly charged hard spheres such that they are interacting via excluded volume and Coulomb forces which are reduced by the dielectric constant ϵ of

the solvent. The two species of charged colloids have a mesoscopic hardcore diameter σ_A (resp. σ_B) and a total charge $Z_A e$ (resp. $Z_B e$) while all microions are monovalent with a charge e (e denoting the electron charge) and a microscopic hardcore diameter σ_c. For finite salt concentrations, there are both counter- and coions in the solution and the microscopic core of oppositely charged microions is needed to prevent the system from the Coulomb collapse. The averaged concentration of added salt is denoted with n_s. The salt is always monovalent. The system is kept at room temperature T such that the Bjerrum length for the microions is $\lambda_B = e^2/\epsilon k_B T = 7.8$Å with $\epsilon = 80$ the dielectric constant of water at room temperature.

A cubic simulation box of edge length L with periodic boundary conditions is used containing two macroions and the following three cases are studied separatedly: i) two A macroions, ii) two B macroions, and iii) one A and one B macroion. The two macroions are placed along the room diagonal of the simulation box and possess a fixed central distance r. At fixed macroion positions, the microions are moved by constant temperature molecular dynamics and the averaged force F acting on the two macroions is calculated. The latter fulfills Newton's third law. For more technical details we refer to the Refs. [49, 50, 54, 55, 56, 57]. Then the distance r is varied and force-distance curve $F(r)$ is gained.

Inspired by the DLVO expression (1), we anticipate that the screening length will not differ much in the three cases i), ii), iii) and that it will be comparable to the Debye-Hückel expression. This assumption will be tested and justified later by a many macroion simulation reported in Section III. Therefore we adjust the box length in the three cases in order to reproduce the same Debye-Hückel screening length (2).

Results for the distance-resolved forces $F(r)$ are shown in Figures 1–3 for the three cases i), ii), and iii) for extremely dilute macroion suspension with a packing fraction $\eta = 0.005$. Such dilute case is chosen to diminish the boundary effects of the simulation box on the interaction forces. The parameters used are σ_A=1220 Å, σ_B=680Å, $Z_A = 580$, and $Z_B = 330$. The prescribed screening is $\kappa_D \sigma_A$= 0.8 corresponding to box lengths of $L = 6.24\sigma_A$ (for i)), $L = 5.72\sigma_A$ (for ii)), and $L = 6.0\sigma_A$ (for iii)). The obtained data for the distance-resolved forces $F(r)$ were fitted with the Yukawa expression $Z_{ij}^{*\,2} e^2/(\epsilon r)(1/r + \kappa)\exp(-\kappa r)$ with $(ij) = (AA), (AB), (BB)$. The screening parameter κ and the three effective charge numbers Z_{AA}^*, Z_{BB}^*, and Z_{AB}^* are used as fit parameters. We obtain $\kappa\sigma_A = 0.81$ (very close to its Debye-Hückel expression) and effective charge numbers of Z_{AA}^*=470, Z_{BB}^*=260, and Z_{AB}^*=330 such that the nonadditivity parameter is negative:

$$\Delta = \left(Z_{AB}^*\right)^2 / \left(Z_{AA}^* Z_{BB}^*\right) - 1 = -0.11 \tag{4}$$

In a similar manner we calculate the interaction forces and Yukawa fitting parameters for another packing fraction $\eta = 0.017$ at which the images of macroions in neighboring cells start to affect the long-range macroion-macroion interactions. We obtain $\kappa_D \sigma_A = 1.15$ and effective charge numbers of Z_{AA}^*=505, Z_{BB}^*=265, and Z_{AB}^*=342 such that the nonadditivity parameter is Δ=-0.13.

The results for extreme dilute $\eta = 0.005$ and dilute $\eta = 0.017$ cases shown in Figures 1–3 reveal that first of all, the Yukawa expression for the forces is an excellent fit over the relevant distance range explored. Moreover, while the screening parameter is very close to its Debye-Hückel expression, the nonadditivity of 11–13 percent is significant.

Next we explore the dependence of Δ on the charge asymmetry $\alpha = Z_A/Z_B$ by changing it in the range from 0 to 1 while keeping the size asymmetry σ_A/σ_B=1.8 unchanged. In detail, we consider the B-charges Z_B=0, 100, 330, 580 with fixed $Z_A = 580$ and $\kappa_D\sigma_A$=0.8. Using the same simulation technique and fitting procedure, we extract the nonadditivity parameter Δ according to Eq.(4). The results are presented in Figure 4. The nonadditivity parameter Δ shows a clear non-monotonicity as a function of Z_B starting from positive values and turning to negative ones and back to positive ones as Z_B is increasing. For $Z_B = 0$, the BB interaction is small, but the AB interaction has still a repulsive contribution from entropic contact force [51] which drives Δ altogether towards a positive value. The other cases are less intuitive and we do not have a simple argument for the sign of Δ.

We have finally considered also the case of size-symmetric ($\sigma_A = \sigma_B$) but charge-asymmetric Z_A/Z_B=1.76 macroions at a fixed screening length of $\kappa_D\sigma_A = 0.8$. Here, the nonadditivity parameter Δ was found to be -0.01, much smaller than for the corresponding size-asymmetric case with $\sigma_A/\sigma_B = 1.8$. Hence size-asymmetry appears to be the more crucial input for the nonadditivity.

3. Simulations with many macroions

Let us now turn to a many body simulation of the primitive model in a cubic cell containing altogether $N = N_A + N_B = 24$ macroions with different compositions $X = N_B/(N_A + N_B)$. The simulation box contains also $N_c = N_AZ_A + N_BZ_B$ oppositely charged counterions, and N_s salt ion pairs. The other parameters are as before if not otherwise stated. Six different macroion packing fractions were considered: η= 0.017, 0.034, 0.12, 0.16, 0.23, 0.3. For all simulations the salt concentration was kept constant at n_s=4×10^{-6} mol/l. Now both the microions and the macroions are moved by constant temperature molecular dynamics. A simulation snapshot is shown in Figure 5. After equilibration, we stored 200 statistically independent macroion configurations for each run. For each stored configuration, we averaged the total forces $\vec{F}_i$ (i=1, N) acting on the ith macroion over the microionic degrees of freedom. These forces are clearly many-body forces, in general. Following the idea of Ref. [53], we assign an optimal effective pair interaction by fitting all forces $\vec{F}_i$ in all stored configurations by the same pairwise Yukawa interaction. As in Section II, the four fitting parameters are κ_D and the three effective charge numbers Z^*_{AA}, Z^*_{BB}, and Z^*_{AB} which determine the nonadditivity Δ directly.

The results of the optimal fit for Δ, Z^*_{AA}, Z^*_{BB}, and $\kappa_D\sigma_A$ are shown in Figures 6–9 as a function of the varied macroion volume fraction η for three different compositions

$X = 1/3, 1/2, 2/3$.

The nonadditivity shown in Figure 6 is clearly negative and decreases with increasing packing fraction. This trend can be intuitively understood since asymmetries are amplified if one approaches smaller interparticle distances. A second important conclusion from Figure 6 is that the many-body simulations yield the *same* value for Δ as those obtained from the simulations of pairs in Sect. II. In fact, the value $\Delta = -0.13$ is reproduced at low volume fractions $\eta = 0.017$. The effective charges and screening length deduced from pair macroion simulations for $\eta = 0.017$ perfectly fit the simulation data for many macroions at the same packing fraction η for the macroions. The effective charge numbers Z^*_{AA} and Z^*_{BB} shown in Figures 7 and 8 increase slightly with volume fraction which is the standard trend also for one-component charged suspensions [58, 59]. The screening constant shown in Figure 9 increases with η following the same trend as its Debye-Hückel expression which is also indicated in Figure 9.

4. Simulations using the optimal effective Yukawa interaction

We finally explore the impact of a non-vanishing Δ on the fluid structure of binary charged suspensions. In doing so we make use of the optimal effective Yukawa fit gained in Sect. III and use it as an input in classical coarse-grained binary Yukawa simulations (without any microions). These simulations can be done for much larger systems and we included 1000 A and 1000 B particles at equimolar composition. Two volume fraction are considered, a dilute system with η=0.034 and a dense system where η=0.3.

The effective macroion charge numbers, the screening constant and the nonadditivity parameter were chosen from results described in the previous section. In detail, for the dilute system: Z^*_{AA}= 530, Z^*_{BB}= 269, $\kappa_D\sigma_A$=1.3, Δ=-0.14, while for the dense system, Z^*_{AA}=580, Z^*_{BB}=330, $\kappa_D\sigma_A$=3.4, Δ=-0.2. At these parameters the system is in the fluid phase.

We have calculated the partial pair correlations g_{AA}, g_{BB} and g_{AB} for the large Yukawa substitute system and the smaller system with explicit microions. The results are presented in Figures 10 and 11. There is good agreement for the dilute case demonstrating that the Yukawa fit is reproducing the pair correlations. For the dense system, there is again agreement except for the location of the first peak in $g_{BB}(r)$. This could have to do with finite-size effects of the $N = 24$ primitive model systems which are expected to get more prominent at high packing fractions.

As a reference we have also performed Yukawa simulations with effective interactions based on two effective charges Z^*_{AA} and Z^*_{BB} but where Δ is set to zero, i.e. where ${Z^*_{AB}}^2 = Z^*_{AA}Z^*_{BB}$. The differences in the pair structure are pointing to the importance of nonzero nonadditivity. There are even more deviation of the fluid pair structure when the simple DLVO expression is taken, which significantly overestimates the structure, see the dotted lines in Figures 10 and 11. One of the main conclusions therefore is that one has to be careful if Δ for binary charged suspensions is neglected.

5. Concluding remarks

In conclusion we have determined the non-additivity parameter in binary charged suspensions by primitive model computer simulations with explicit microions and found significant deviations from zero. The sign depends on the actual parameter combination, in particular on the charge asymmetry. This implies that a realistic modelling of charged suspensions on the effective pairwise Yukawa level should incorporate a non-vanishing Δ.

A priori an intuition for the sign of Δ is difficult. Intuition only works in limiting cases. For example, in the depletion limit of many small macroions and few big ones, there is attraction between the big ones which would result in a positive Δ.

In the future, more detailed investigation are planned to explore the full parameter space better. It would be interesting to calculate the effective interaction in the solid phase relative to the fluid crystalline phase.

In inhomogeneous situations like sedimentation in a gravitational field, binary suspensions have been examined by primitive model computer simulations [60] and a simple binary Yukawa pairwise interaction model was found to be inappropriate [61]. Since in our bulk simulation the pairwise Yukawa model was a good fit, we expect that this is due to the density gradient in the system but this will require more detailed studies.

Binary suspension can be prepared in a controlled way [62, 63] and their structural correlation, dynamics and phase diagrams can be explored. Depending on the size and charge ratio different freezing diagrams (azeotropic, spindle, eutectic) [64, 65, 66, 67] have been obtained in the experiments. Since the nonadditivity Δ depends on the composition, this might point to the fact that details of the variation of Δ with composition and also with the phases itself (fluid or crystal) determines the shape of the freezing diagrams. Finally it would be interesting to study nonadditivity effects in charged mixtures of rods [68] or rod and sphere mixtures. It would also be interesting to explore the effect of multivalent counterions which could lead to mutual attraction [50, 69].

Acknowledgments

We thank T. Palberg and A. V. Ivlev for helpful discussions. This work was supported by the DFG via the SFB TR6 (project D1).

[1] G. Tammann, Ann. d. Physik. **40**, 237 (1913).
[2] J. Hafner, *From Hamiltonians to Phase Diagrams* (Springer, Berlin, 1987).
[3] G. Gompper and M. Schick, *Soft Matter, Vol. 2: Complex Colloidal Suspensions* (WILEY-VCH Verlag GmbH and Co. KGaA, Weinheim, 2006).
[4] S. Pronk and D. Frenkel, Phys. Rev. Lett. **90**, 255501 (2003).
[5] H. Xu and M. Baus, J. Phys: Condens. Matter **4**, L663 (1992).
[6] M. D. Eldridge, P. A. Madden, and D. Frenkel, Nature **365**, 35 (1993).
[7] P. Bartlett, R. H. Ottewill, and P. N. Pusey, Phys. Rev. Lett. **68**, 3801 (1992).

[8] M. E. Leunissen, C. G. Christova, A. P. Hynninen, C. P. Royall, A. I. Campbell, A. Imhof, M. Dijkstra, R. van Roij, and A. van Blaaderen, Nature **437**, 235 (2005).
[9] A. P. Hynninen, C. G. Christova, R. van Roij, A. van Blaaderen, and M. Dijkstra, Phys. Rev. Lett. **96**, 138308 (2006).
[10] L. Assoud, R. Messina, and H. Löwen, Europhys. Letters **80**, 48001 (2007).
[11] J. Fornleitner, F. Lo Verso, G. Kahl and C. N. Likos, Soft Matter, **4** 480 (2008).
[12] L. Assoud, R. Messina, H. Löwen, J. Chem. Phys. **129**, 164511 (2008).
[13] J.-P. Hansen, H. Löwen, Annual Reviews of Physical Chemistry, **51**, 209 (2000).
[14] Y. Levin, Reports on Progress in Physics **65**, 1577 (2002).
[15] R. Messina, J. Phys.: Condensed Matter **21**, 113102 (2009).
[16] J. M. Mendez-Alcaraz, B. D'Aguanno, R. Klein, Physica A, **178**, 421 (1991).
[17] R. Krause, B. D'Aguanno, J. M. Mendez-Alcaraz, R. Klein, J. Phys.: Condensed Matter **3**, 4459 (1991).
[18] H. Löwen, J. P. Hansen, P. A. Madden, J. Chem. Phys. **98**, 3275 (1993).
[19] H. Löwen, P. A. Madden, J. P. Hansen, Phys. Rev. Letters **68**, 1081 (1992).
[20] H. Löwen, E. Allahyarov, J. Phys.: Condensed Matter **10**, 4147 (1998).
[21] J. Z. Wu, D. Bratko, H. W. Blanch, J. M. Prausnitz, J. Chem. Phys. **113**, 3360 (2000). J. Phys.: Condensed Matter **10**, 4147 (1998).
[22] D. Reinke, H. Stark, H. H. von Grünberg, A. B. Schofield, G. Maret, U. Gasser, Phys. Rev. Letters **98**, 038301 (2007).
[23] C. Russ, M. Brunner, C. Bechinger, H. H. Von Grünberg, Europhysics Letters **69**, 468 (2005).
[24] T. Kreer, J. Horbach, A. Chatterji, Phys. Rev. E **74**, 021401 (2006).
[25] E. Trizac, L. Bocquet, M. Aubouy, H. H. von Grünberg, Langmuir **19**, 4027 (2003).
[26] A. Torres, G. Téllez, R. van Roij, J. Chem. Phys. **128**, 154906 (2008).
[27] R. Roth, R. Evans, A. A. Louis, Phys. Rev. E **64**, 051202 (2001).
[28] A. A. Louis, R. Roth, J. Phys.: Condensed Matter **13**, L777 (2001).
[29] G. Pellicane, F. Saija, C. Caccamo, P. V. Giaquinta, J. Chem. Phys. **110**, 4359 (2006).
[30] N. Hoffmann, F. Ebert, C. N. Likos, G. Maret, and H. Löwen, Phys. Rev. Lett. **97**, 078301 (2006).
[31] P. Hopkins, A. J. Archer, R. Evans, J. Chem. Phys. **124**, 054503 (2006). Phys. **110**, 4359 (2006).
[32] P. Hopkins, A. J. Archer, R. Evans, J. Chem. Phys. **129**, 214709 (2008).
[33] O. S. Vaulina and I. E. Dranzhevskii, Plasma. Phys. Reports **33**, 494 (2007).
[34] G. J. Kalman, P. Hartmann, Z. Donko, and M. Rosenberg, Phys. Rev. Lett. **92**, 065001 (2004).
[35] K. R. Sütterlin, A. Wysocki, A. V. Ivlev, C. Räth, H. M. Thomas, M. Rubin-Zuzic, W. J. Goedheer, V. E. Fortov, A. M. Lipaev, V. I. Molotkov, O. F. Petrov, G. E. Morfill, H. Löwen, Phys. Rev. Letters **102**, 085003 (2009).
[36] N. Kikuchi, J. Horbach, EPL **77**, 26001 (2007).
[37] A. Carre, L. Berthier, J. Horbach, S. Ispas, W. Kob, J. Chem. Phys. **127**, 114512 (2007).
[38] A. A. Louis, E. Allahyarov, H. Löwen, and R. Roth, Phys. Rev. E **65**, 061407 (2002).
[39] E. Schöll-Paschinger and G. Kahl, J. Chem. Phys. **118**, 7414 (2003).
[40] P. Hopkins, A. J. Archer, and R. Evans, J. Chem. Phys. **124**, 054503 (2006).
[41] J. Köfinger, N. B. Wilding, and G. Kahl, J. Chem. Phys. **125**, 234503 (2006).
[42] H. Löwen, J. P. Hansen, J. N. Roux, Phys. Rev. A **44**, 1169 (1991).
[43] M. A. Chavez-Rojo and M. Medina-Noyola, Physica A **366**, 55 (2006).
[44] N. Kikuchi and J. Horbach, Europhys. Letters **77**, 26001 (2007).
[45] M. A. Chavez-Rojo, R. Juarez-Maldonado, M. Medina-Noyola, Phys. Rev. E **77**, 040401(R) (2008).
[46] R. Juarez-Maldonado, M. Medina-Noyola, Phys. Rev. E **77**, 051503 (2008).
[47] G. Salin and D. Gilles, J. Phys. A: Math. Gen. **17**, 4517 (2006).
[48] A. V. Ivlev, S. K. Zhdanov, H. M. Thomas, G. E. Morfill, EPL (in press).
[49] I. D'Amico, H. Löwen, Physica A **237**, 25 (1997).
[50] E. Allahyarov, I. D'Amico, H. Löwen, Phys. Rev. Letters **81**, 1334 (1998).
[51] E. Allahyarov, H. Löwen, and S. Trigger, Phys. Rev. E **57**, 5818 (1998).

[52] E. Allahyarov, I. D'Amico, and H. Löwen, Phys. Rev. E **90**, 3199 (1999).
[53] H. Löwen, G. Kramposthuber, Europhys. Letters **23**, 637 (1993).
[54] H. Löwen, A. Härtel, A. Barreira-Fontecha, H. J. Schöpe, E. Allahyarov, T. Palberg, J. Phys.: Condensed Matter **20**, 404221 (2008).
[55] E. Allahyarov, H. Löwen, A. A. Louis, J.-P. Hansen, Europhys. Letters **57**, 731 (2002).
[56] E. Allahyarov, H. Löwen, A. A. Louis, J.-P. Hansen, Phys. Rev. E **67**, 051404 (2003)
[57] E. Allahyarov, E. Zaccarelli, F. Sciortino, P. Tartaglia, H. Löwen, Europhysics Letters **78**, 38002 (2007).
[58] A. Diehl, M. C. Barbosa, Y. Levin, Europhysics Letters **53**, 86 (2001).
[59] A. R. Denton, J. Phys.: Cond. Matter **20**, 494230 (2008).
[60] A. Esztermann, H. Löwen, Europhys. Letters **68**, 120 (2004).
[61] A. Torres, A. Cuetos, M. Dijkstra, R. van Roij, Phys. Rev. E **77**, 031402 (2008).
[62] G. H. Koenderink, H. Y. Zhang, M. P. Lettinga, G. Nägele, A. P. Philipse, Phys. Rev. E **64**, 022401 (2001).
[63] A. Stipp, T. Palberg, Phil. Mag. Letters **87**, 899 (2007).
[64] W. J. Hunt, C. F. Zukoski, J. Colloid Interface Sci. **210**, 332 (1999).
[65] A. Meller, J. Stavans, Phys. Rev. Letters **68**, 3645 (1992)
[66] P. Wette, H. J. Schöpe, T. Palberg, J. Chem. Phys. **122**, 144901 (2005).
[67] N. Lorenz, J. N. Liu, T. Palberg, Colloids and Surfaces A **319**, 109 (2008).
[68] H. Löwen, J. Chem. Phys. **100**, 6738 (1994).
[69] E. Allahyarov, G. Gompper, H. Löwen, Phys. Rev. E **69**, 041904 (2004).

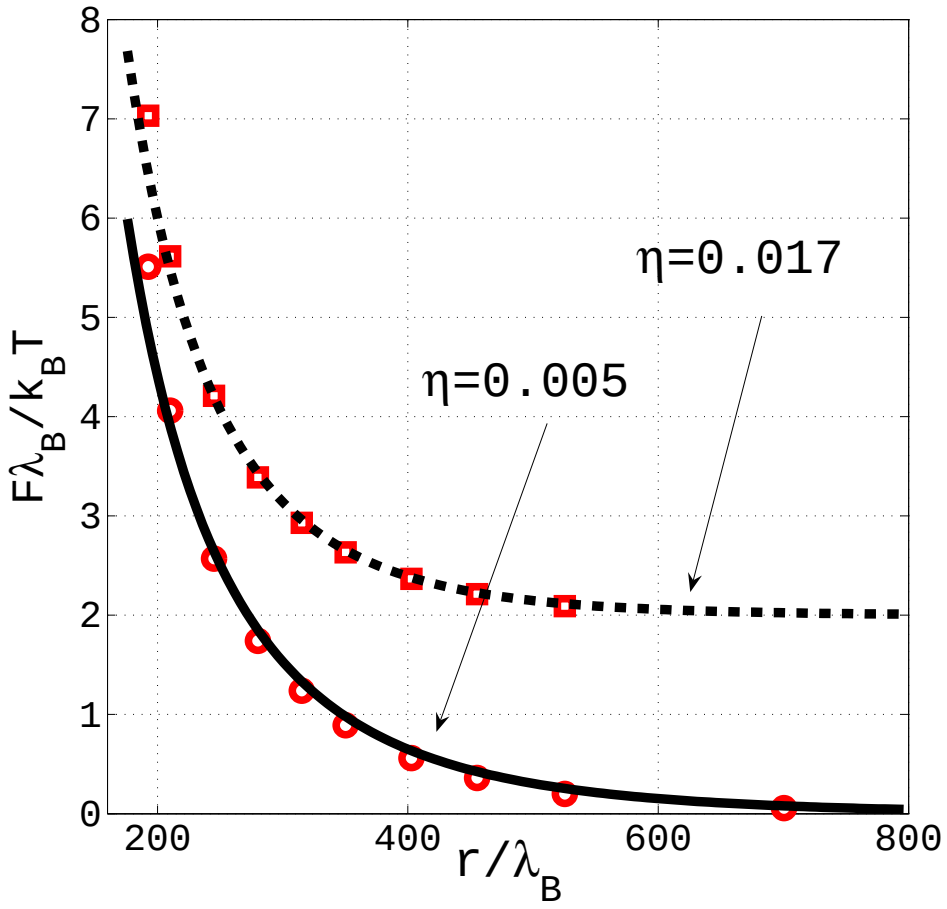

Figure 1. (Color online) Dimensionless interaction force $F\lambda_B/(k_BT)$ for case i) (AA macroion pair) as a function of dimensionless separation distance r/λ_B. Symbols denote the simulation data, the full curves are the Yukawa fit for two macroion packing fractions $\eta = 0.005$ (soilid line) and $\eta = 0.017$ (dashed line, shifted upward). The fit data are given in the text.

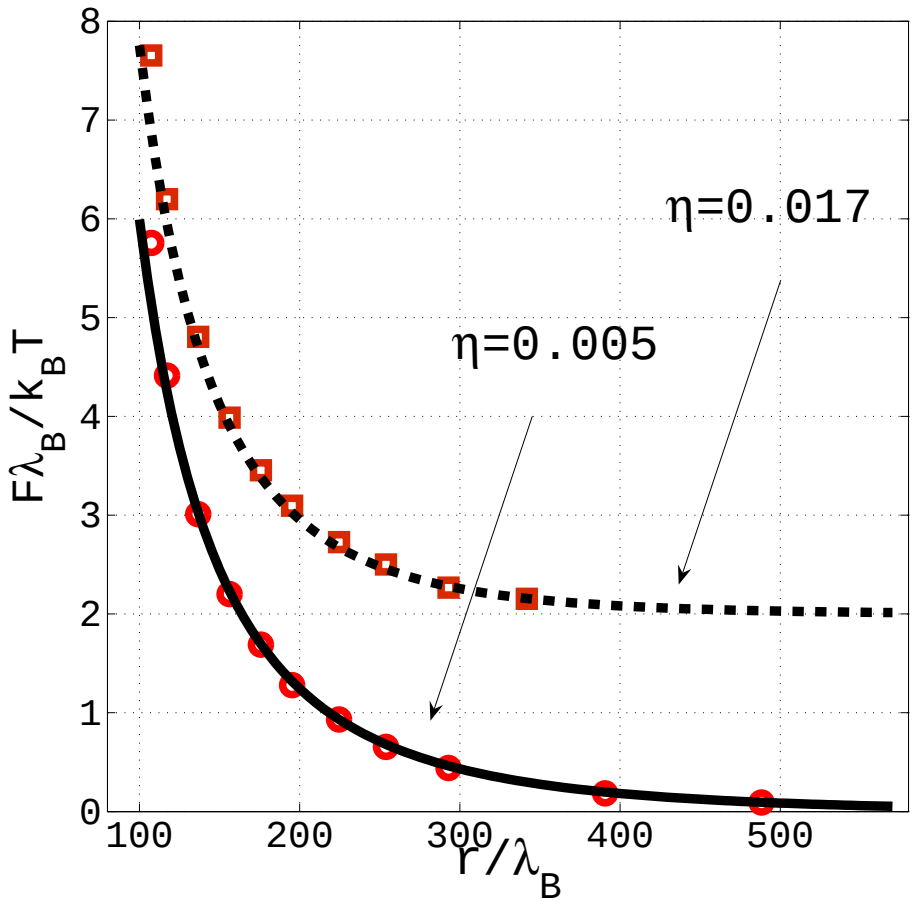

Figure 2. (Color online) Dimensionless interaction force $F\lambda_B/(k_BT)$ for case ii) (BB macroion pair) as a function of a dimensionless separation distance r/λ_B. Symbols denote the simulation data, the full curves are the Yukawa fit for two macroion packing fractions $\eta = 0.005$ (solid line) and $\eta = 0.017$ (dashed line, shifted upward). The fit data are given in the text.

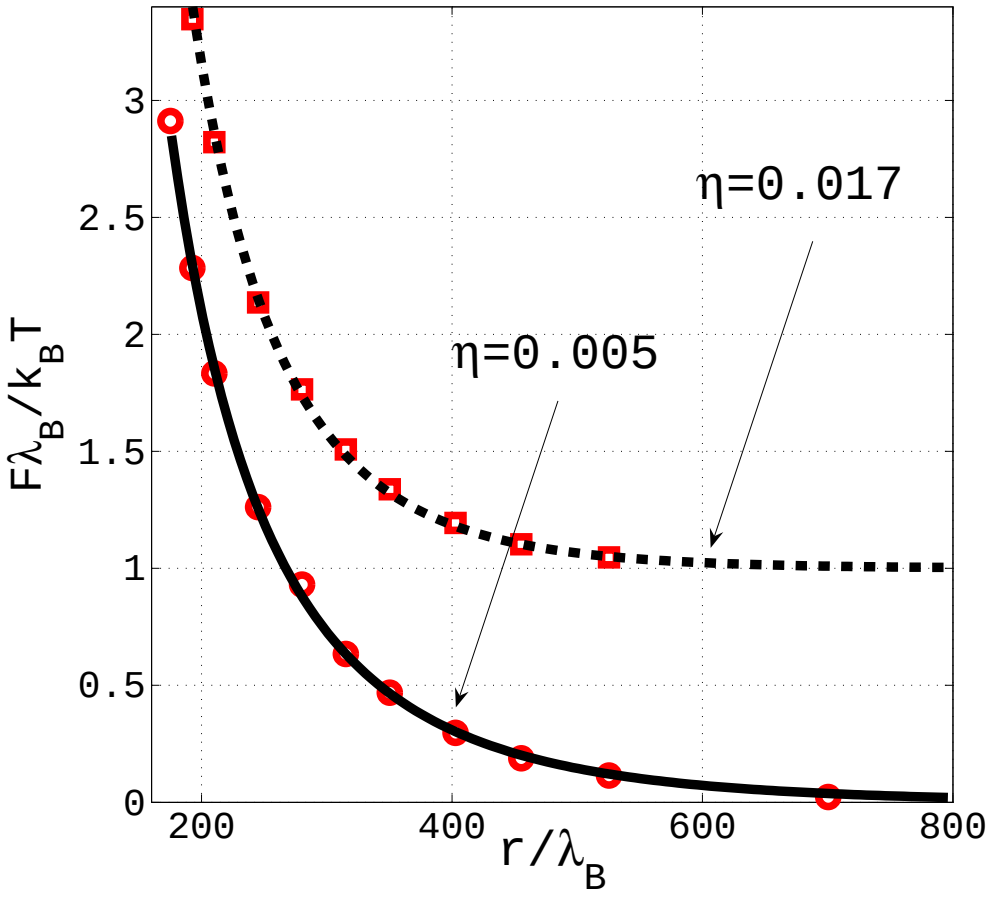

Figure 3. (Color online) Dimensionless interaction force $F\lambda_B/(k_BT)$ for case iii) (pair of A and B macroion) as a function of a dimensionless separation distance r/λ_B. Symbols denote the simulation data, the full curves are the Yukawa fit for two macroion packing fractions $\eta = 0.005$ (solid line) and $\eta = 0.017$ (dashed line, shifted upward). The fit data are given in the text.

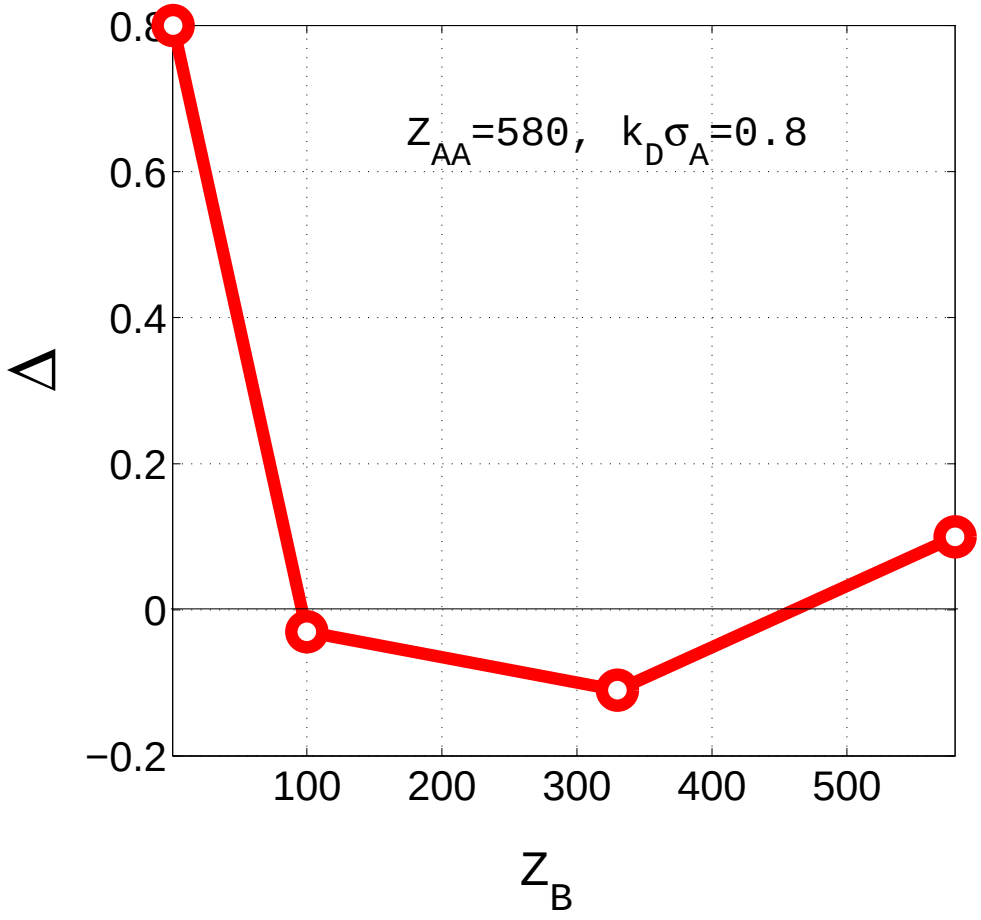

Figure 4. (Color online) Nonadditivity parameter Δ for different charges Z_B at a fixed charge $Z_A = 580$.

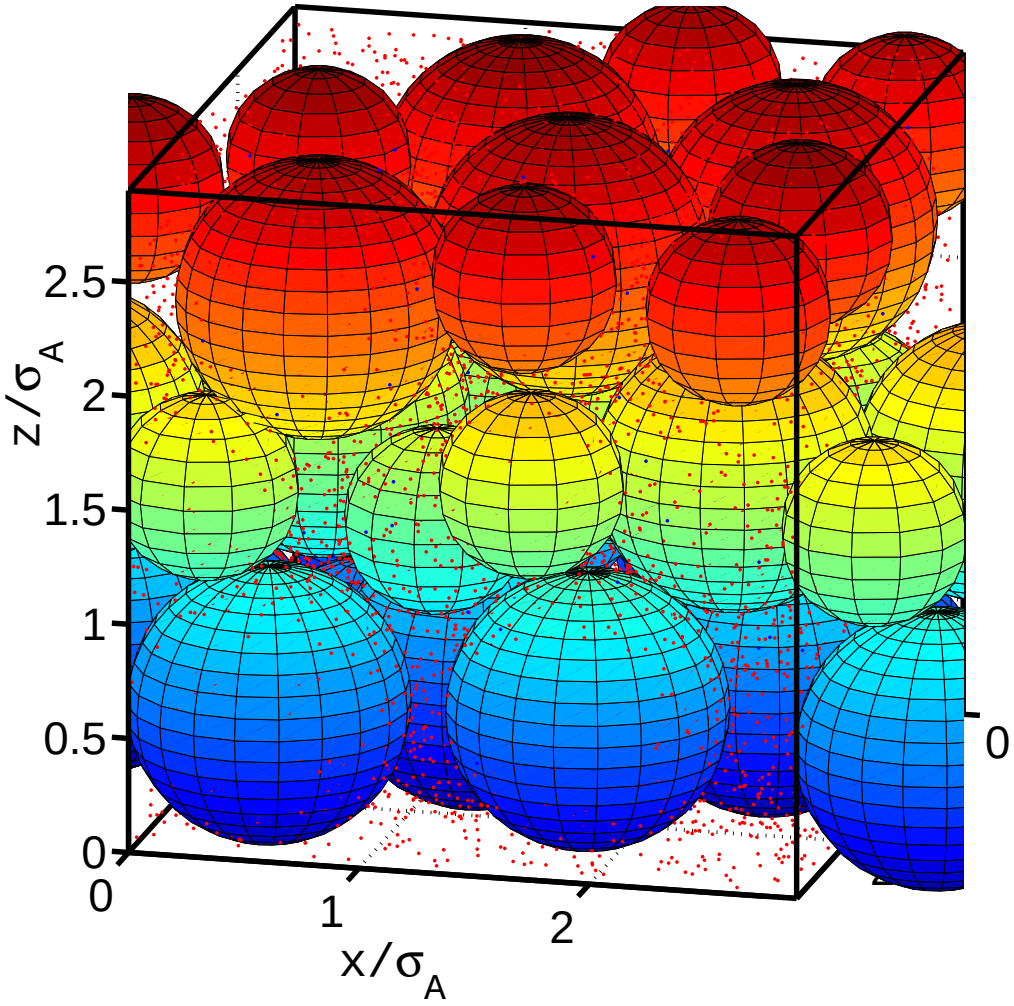

Figure 5. (Color online) Full system snapshot picture for 24 macroions with equimolar composition $X = 1/2$. The system size is 2.9 σ_A at a total packing fraction of η=0.3. The positively charged counter- and salt ions are shown as red dots, while the negatively salt ions are shown as blue dots. A vertical color gradient has been used for macroion positions along the z-axis. The parameters are: Z_A=580, Z_B=330.

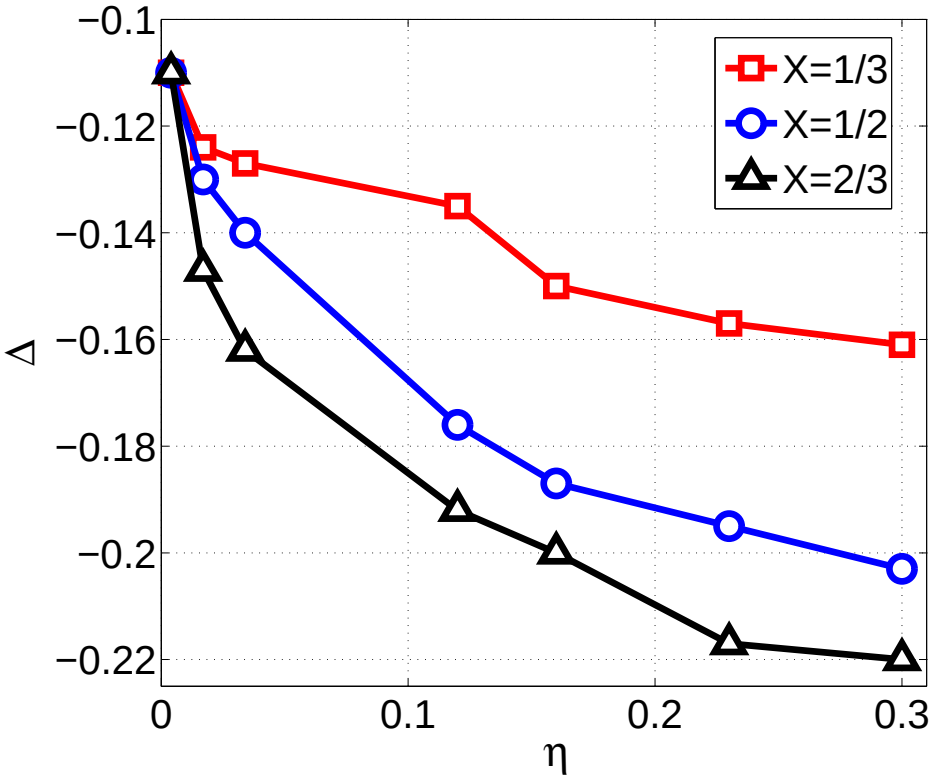

Figure 6. (Color online) Nonadditivity parameter Δ as a function of a total macroion packing fraction η for three different compositions $X = 1/3, 1/2, 2/3$.

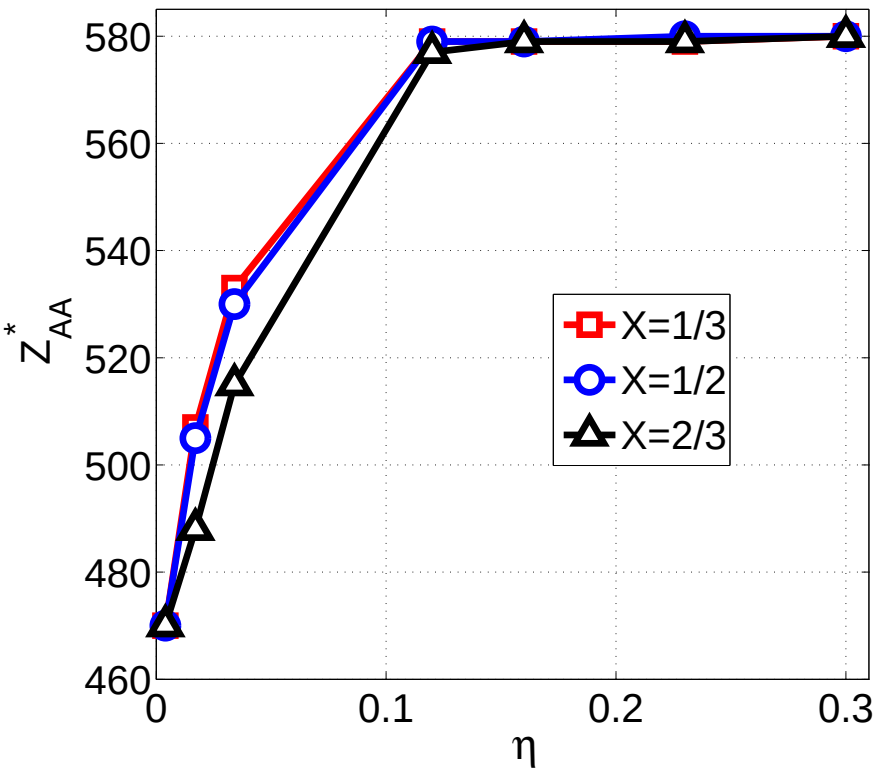

Figure 7. (Color online) Optimal effective AA charge number Z^*_{AA} as a function of a total macroion packing fraction η for three different compositions $X = 1/3, 1/2, 2/3$.

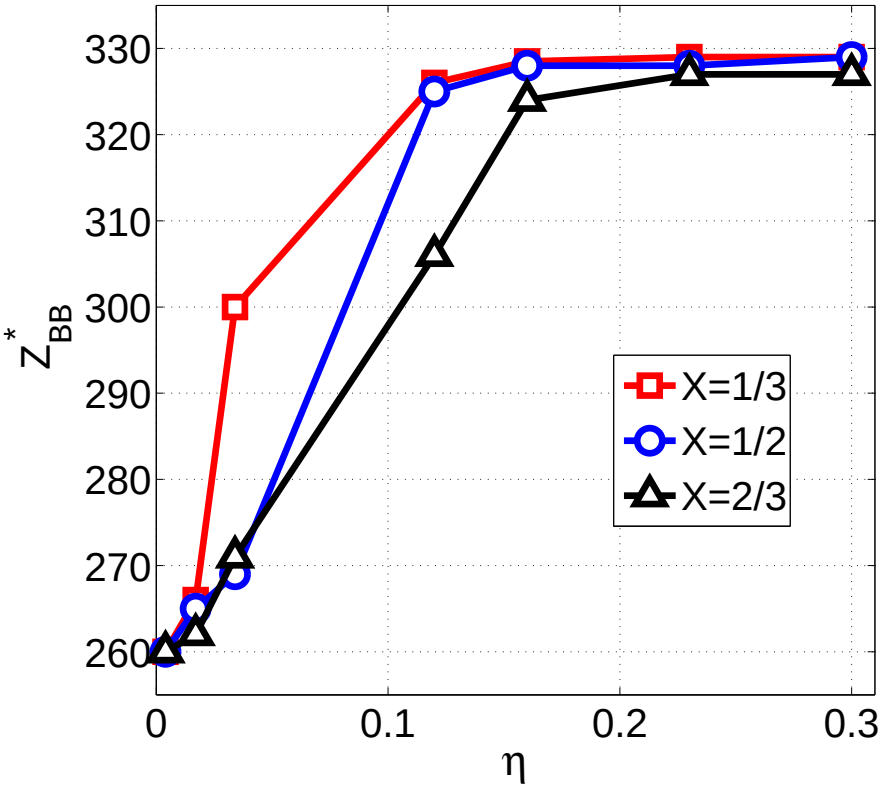

Figure 8. (Color online) Optimal effective BB charge number Z^*_{BB} as a function of a total macroion packing fraction η for three different compositions $X = 1/3, 1/2, 2/3$.

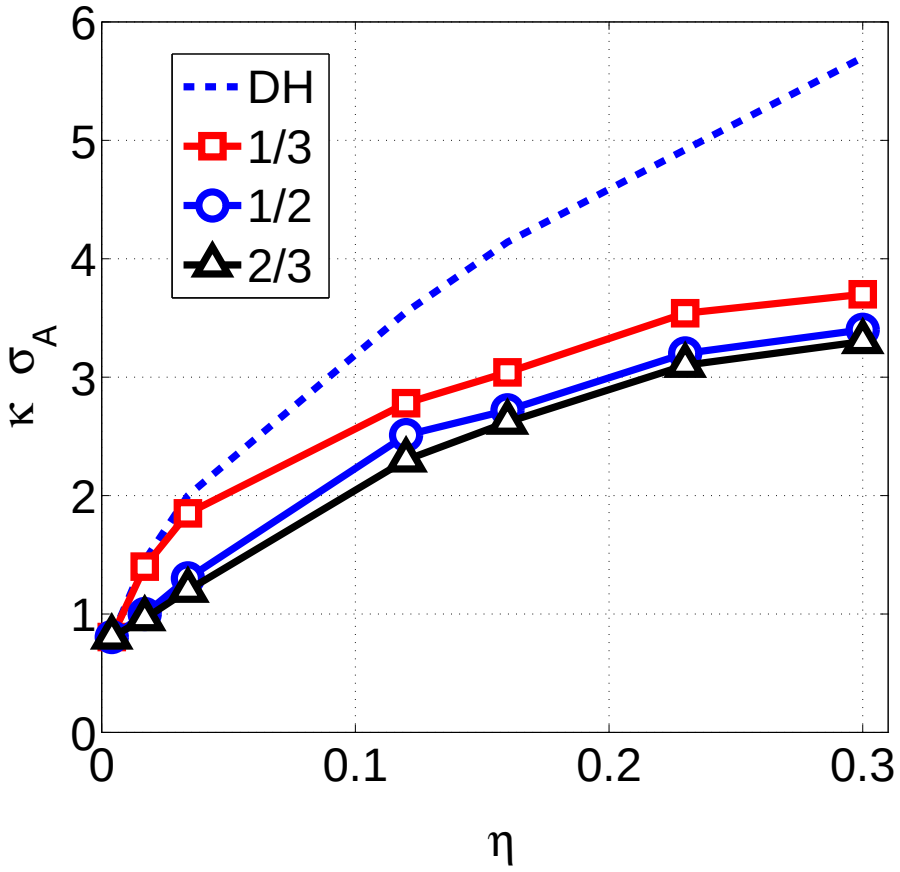

Figure 9. (Color online) Optimal screening parameter $\kappa\sigma_A$ as a function of a total macroion packing fraction η for three different compositions $X = 1/3, 1/2, 2/3$. The dashed line is the Debye-Hückel value of screening in the simulated system according to Eq.(2) in the text.

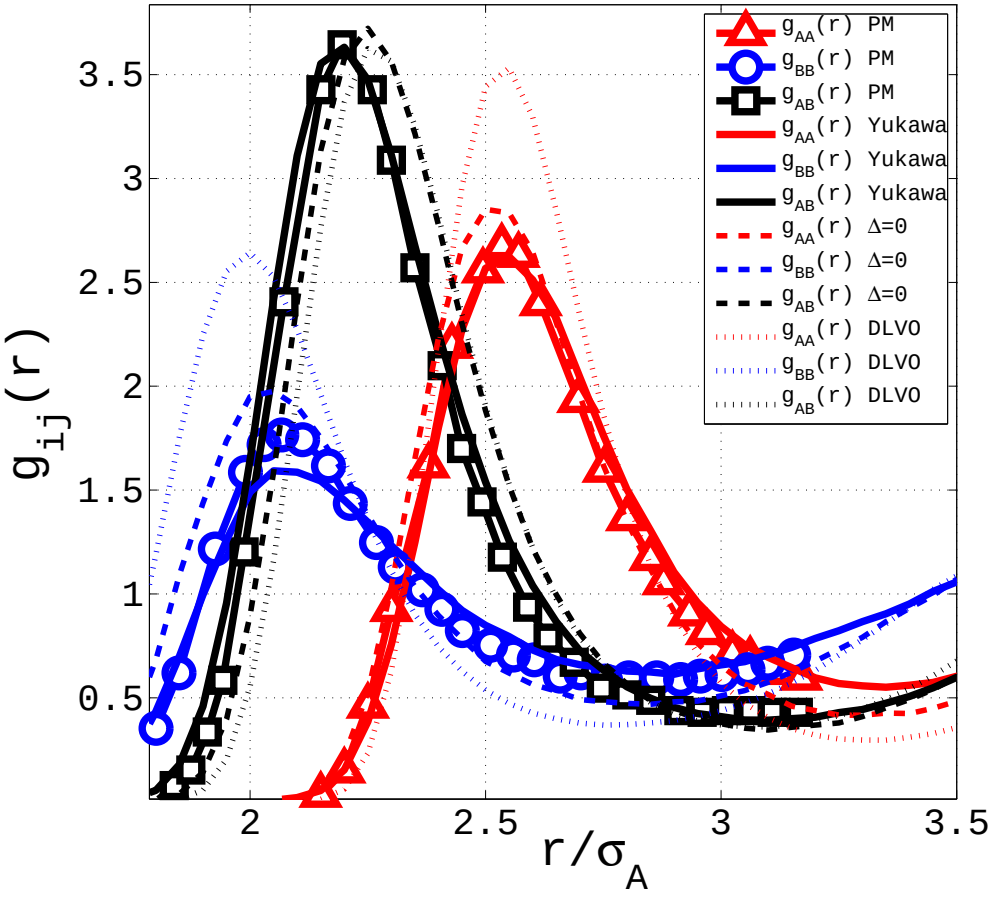

Figure 10. (Color online) Partial macroion-macroion pair correlation functions for both the full primitive model (symbols) and the substitute Yukawa system (full lines) for a total packing fraction η=0.034 at composition $X = 1/2$. The Yukawa simulations were carried for Δ=-0.14, $\kappa_D\sigma_A$=1.3, Z^*_{AA}=530, Z^*_{BB}=269. The additive Yukawa system results for Δ=0 and the same $\kappa_D\sigma_A$, Z^*_{AA}, Z^*_{BB} are given as dashed lines. The DLVO predictions are included as dotted lines.

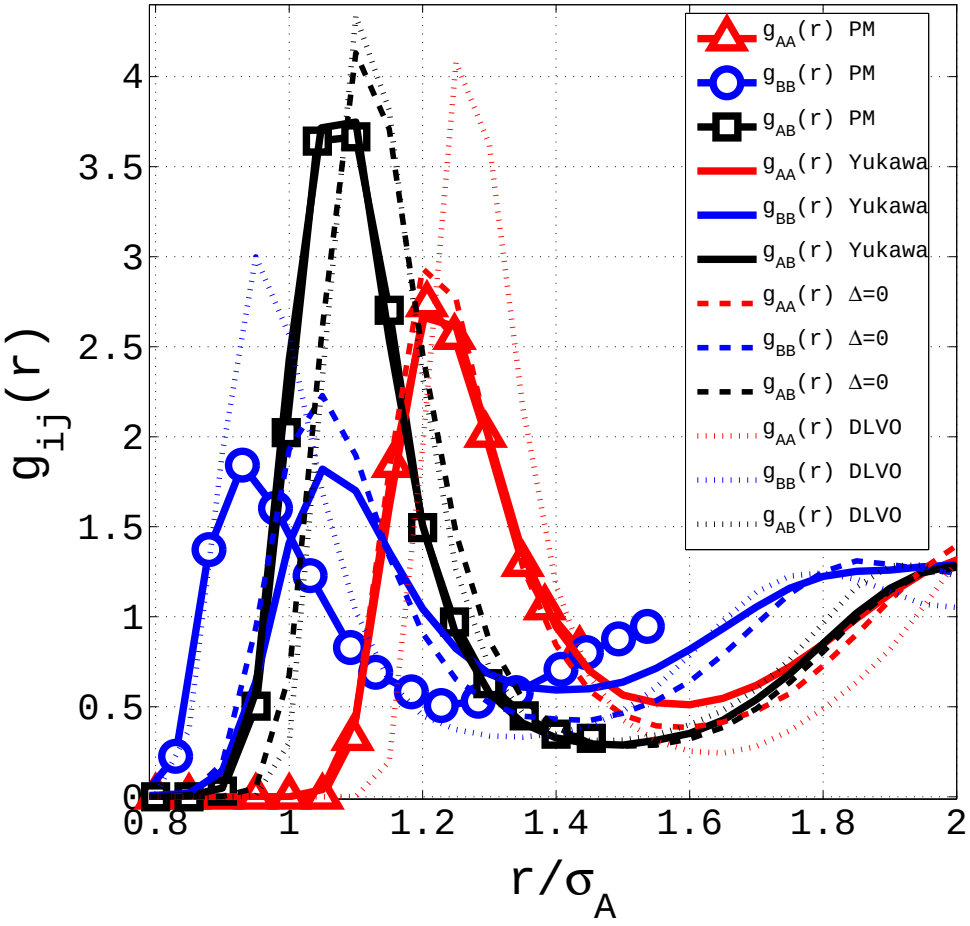

Figure 11. (Color online)Partial macroion-macroion pair correlation functions for both the full primitive model (symbols) and the substitute Yukawa system (full lines) for a total packing fraction η=0.3 at composition $X = 1/2$. The Yukawa simulations were carried for Δ=-0.2, $\kappa_D\sigma_A$=3.4, Z^*_{AA}=580, Z^*_{BB}=330. The additive Yukawa system results for Δ=0 and the same $\kappa_D\sigma_A$, Z^*_{AA}, Z^*_{BB} are given as dashed lines. The DLVO predictions are included as dotted lines.